A search for flavour changing neutral currents involving a top quark and a Z boson, using the data collected by the CMS collaboration at a centre of mass of 13 TeV

Van Parijs, Isis

Proefschrift ingediend met het oog op het behalen van de academische graad Doctor in de Wetenschappen.

Published in Faculteit Wetenschappen & Bio-ingenieurswetenschappen
Vrije Universiteit Brussel
At 1. June 2017.

Responsible Contact: I. Van Parijs
Intitute for High Energy Physics

First Referee: Prof. Dr. J. D'Hondt
Date of Hand-in: 1 June 2017
Date of Defense: 1 October 2017

Contents

1 Theoretical bases

Experimental setup 2

The main objective of the Large Hadron Collider (LHC) was the search for the Brout-Englert-Higgs boson (or scalar boson). It was known from the Linear Electron Positron and Tevatron experiments that the scalar boson mass had to be larger than 114 GeV[1, 2], and smaller than around 1 TeV due to unitarity and perturbativity constraints [3]. On top of this, the search of supersymmetry or dark matter where part of the motivation for building the LHC. Since the start of its operation, the LHC is pushing the boundaries of the Standard Model, putting the best limits on physics beyond the Standard Model as well as precision measurements of the parameters of the Standard Model. One such an accomplishment is the discovery the scalar boson in 2012 by the two largest experiments at the LHCı[4, 5].

In the first part of this chapter, the LHC and the acceleration process for protons to reach their design energies is discussed. The second part presents the Compact Muon Solenoid.

2.1 The Large Hadron Collider

The LHC has started its era of cutting edge science on 10 September 2008 [6] after approval by the European Organisation of Nuclear Research (CERN) in 1995 [7]. Installed in the previous Large Electron Positron collider (LEP) tunnels, the LHC consists of a 26.7 km ring, that is installed between 45 and 170 m under the French-Swiss border between Cessy (France) and Meyrin (Switzerland). Built to study rare physics phenomena at high energies, the LHC has the possibility to accelerate two type of particles - protons or ions Pb^{45+} - and provides collisions at four points of interaction. At the interaction points, experiments are installed in order to study the collisions.

As can be seen in figure 2.1, the LHC is last element in a chain of creation, injection and acceleration of protons. Protons are obtained by ionising hydrogen and injected in a linear accerator (LINAC 2), where they obtain an energy of 50 MeV. They continue to the proton synchrotron booster (PSB or Booster), where the proton packets are accelerated to 1.4 GeV and are split up in twelve. The proton synchrotron (PS) increases their energy to 25 GeV before handing the protons to the super proton synchrotron (SPS), where the proton reach an energy of 450 GeV. Each accelerator ring increases in radius in order to reduce the energy loss of the protons by synchrotron radiation. This energy loss is proportional to the fourth power of the

proton energy and inversely proportional to the bending radius. The protons are then injected into opposite directions into the LHC, where they are accelerated to 3.5 TeV (in 2010 and 2011), 4 TeV (in 2012 and 2013) or 6.5 TeV (in 2015 and 2016) [8]. Before the start up of the LHC in 2010, the previous energy record was held by the Tevatron collider at Fermilab, colliding proton with antiprotons at $\sqrt{s} = 1.96$ TeV.

The beam has a bunch structure obtained by the injection scheme and properties of the dump system. These bunches are obtained in the PS with 25 ns spacing. The operation of accelerating and transfering to the LHC is repeated 12 times for each counter-rotating beam. When completly filled, the LHC nominally contains 32808 bunches (FIXME) of approximatley 10^{11} protons.

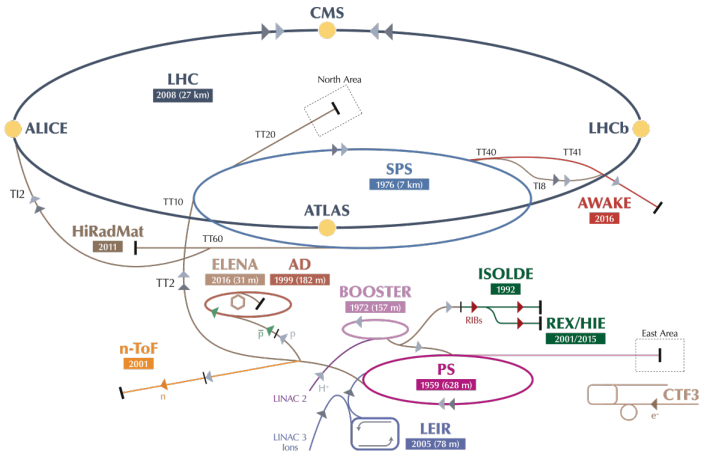

Figure 2.1: Schematic representation of the accelerator complex at CERN [9]. The LHC (dark blue) is the last element in chain of accelerators. Protons are successively accelerated by LINAC 2, the Booster, the Proton Synchrotron (PS) and the Super Proton Synchrotron (SPS) before entering the LHC.

The LHC is home to seven experiments that are placed on an interaction point:

- A Toroidal LHC ApparatuS (ATLAS [10]) and the Compact Muon Solenoid (CMS [11]) experiments are the two general purpose detectors at the LHC. They both have a hermetic, cylindrical structure and were designed to search for new physics phenomena as well as precision measurements of the Standard Model. The existence of two distinct experiments allows cross-confirmation for any discovery.

- A Large Ion Collider Experiment (ALICE [12]) and the LHC Beauty (LHCb [13]) experiments are focusing on specific phenomena. ALICE studies strongly interacting matter at extreme energy densities where quark-gluon plasma forms from heavy ions (Pb-Pb or p-Pb). LHCb searches for differences between matter and anti matter by means of the b quark, while focussing on CP symmetry violation.

- The forward LHC (LHCf [14]) and the TOTal cross section, Elastic scattering and diffraction dissociation Measurement (TOTEM [15]) experiments are two smaller experiments that

focus on interactions where protons or heavy ions only meet while head on collisions take place. LHCf consists of two parts placed before and after ATLAS and studies particles created at very small angles. TOTEM is placed in the same cavern as CMS and performs precise measurements of the LHC luminosity.

- The Monopoles and Exotics Detector At the LHC (MoEDAL [16]) experiment is situated near LHCb and tries to find magnetic monopoles.

2.1.1 LHC design and operation

The most important quantity at the LHC is the luminosity. This is a measurement of the number of collisions that can be produced in a detector per m^2 and per second. The LHC collisions create a number of events per second given by

$$N_{event} = L\sigma_{event}, \tag{2.1}$$

where σ_{event} is the cross section of the event of interest and L the machine luminosity. This luminosity depends only on the beam parameters and is for a Gaussian beam expressed as

$$L = \frac{1}{4\pi} N_b n_b f_{rev} \frac{N_b}{\epsilon_n} \left(1 + \left(\frac{\theta_c \sigma_z}{2\sigma^*}\right)^2\right)^{\frac{-1}{2}} \frac{\gamma_r}{\beta^*}. \tag{2.2}$$

The number of particles per bunch is expressed by N_b, while n_b is the number of bunches per beam, f_{rev} the revolution frequency, γ_r the relativistic gamma factor, ϵ_n the normalized transverse beam emittance - a quality for the confinement of the beam , β^* the beta function at the collision point - a measurement for the width of the beam, θ_c the angle between the two beams at the interaction point, σ_z the mean lengths of one packet, and σ^* the mean height of one packet. In Equation 2.2, the blue part represents the stream of particles, the red represents the brilliance; and the green part represents the geometric reduction factor due to the crossing angle at the interaction point. Hence, in order to enhance the chances for exploration of rare events and thus enhancing the number of collisions. High beam energies as well as high beam intensities are required.

The peak luminosity for the LHC in 2016 was 10^{34} $1/(m^2\,s)$, which leads to about 1 billion proton interactions per second. This luminosity is not a constant in time. It diminishes due to collisions between the beams, and the interaction of the protons and the particle gas that is trapped in the centre of the vacuum tubes due to the magnetic field. The intern diffusion of the beam degrades the emmitance and therefiore also the luminisity. For this reason, the mean lifetime of a beam inside the LHC is around 15 h. The integrated luminosity - the luminosity provided for a certain time range - recorded by CMS and ATLAS over the year 2016 is given in Figure 2.1.1.

Inside the LHC ring [17], the protons are accelerated by the means of radiofrequenciy cavities, while 1232 dipole magnets of approximately 15 m long, weighing 35 t esure the deflection of the beams. The cross section view of such a dipole is given in Figure 2.4. The two proton beams circulate in opposite direction in separate pipes inside of the magnet. Through the use of a strong electric current in the coils around the beam pipe, magnetic fields are generated and cause

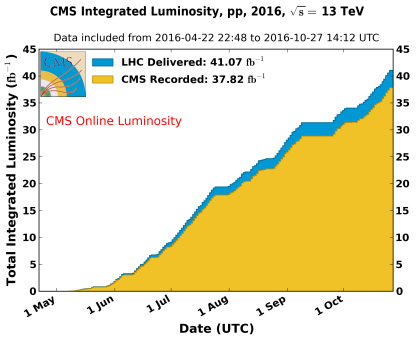

Figure 2.2: Cumulative luminosity measured online versus day delivered to (blue), and recorded by CMS (orange) during stable beams and for proton collisions at 13 TeV centre-of-mass energy in 2016. The delivered luminosity accounts for the luminosity delivered from the start of stable beams until the LHC requests CMS to turn off the sensitive detectors to allow a beam dump or beam studies. FIXME

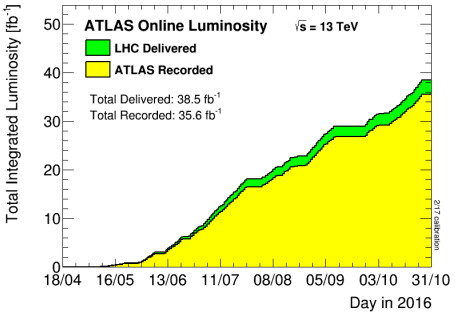

Figure 2.3: Total Integrated Luminosity in 2016 Cumulative luminosity versus time delivered to (green) and recorded by ATLAS (yellow) during stable beams for proton collisions in 2016. The delivered luminosity accounts for luminosity delivered from the start of stable beams until the LHC requests ATLAS to put the detector in a safe standby mode to allow for a beam dump or beam studies. Shown is the luminosity as determined from counting rates measured by the luminosity detectors. FIXME

the protons to bend in the required orbits. In order to get the coil to become superconducting and able to produce - with the aid of an iron return yoke - a strong magnetic field of 8.3 T, the magnet structure is surrounded by a vessel. This vessel is filled with liquid Helium making it possible to cool down the magnet to 1.9 K. In order to get more focussed and stabilised proton beam, other higher-order multipole and corrector magnets are placed along the LHC tunnel.

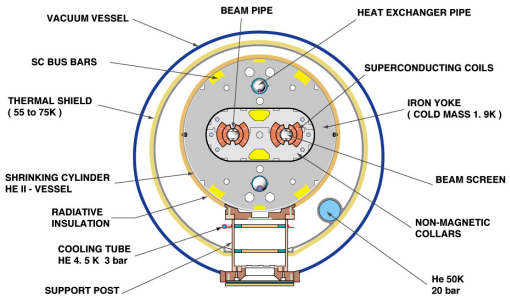

Figure 2.4: Schematic representation of the LHC dipole [18]. Two beam pipes where the proton beams circulate around the LHC ring are shown. The superconducting coils generate a magnetic field of 8.3 Tthat steer the protons in the circular path.

2.2 The Compact Muon Solenoid

At one of the collision points of the LHC, the CMS detector[19–21] is placed. Weighing 14 000 t, This cylindrical detector is about 28.7 m long and 15 m in diameter, weighing around 14 000 t. It has an onion like structure of several specialised detectors and contains a superconducting solenoid with a magnetic field of 3.8 T. The CMS detector is designed in a way that it can address the needs of physics coming from the LHC. Living in a hadronic environment, multi-jet processes produced by the strong interaction are a main source of background for rare physics processes. Therefore, good identification, momentum resolution, and charge determination of muon, electrons and photons is one of the main goals of the CMS detector. Further it provides a good charged particle momentum resolution and reconstruction efficiency in the inner tracker such that for example jets coming from b quarks or tau particles can be identified. Also th electromagnetic resolution for an efficient photon and lepton isolation as well as a good hadronic calorimeter for the missing transverse energy were kept into account while designing CMS.

The LHC provides many collisions in a short amount of time. In order to discriminate between consecutive collisions - known as out of time pile up events - , CMS has to complete the full data acquisition for one collision event before the next one happen (around 50 ns (FIXME)). Furthermore, since the photons are in packets, around 21 (FIXME) inelastic collisions happen every beam crossing. This creates a great amount of background processes in the detector called in time pile up events. Due to this difficult conditions, the detector has a great granularity which on its turn creates a need for huge number of synchronized electronic channels. Furthermore, due to to high flux of particles in the regions close to the beam, the electronics has to be able to endure high radiation.

Before the start of taking collision data for 13 TeV operations on 3 June, CMS had a long shutdown. During this shut down several upgrades were performed:

- Data Acquisition: new architercture, hardware and software
- Trigger Control and Distribution System: new uTCA
- Level-1 Trigger: new calorimeter trigger (uTCA)
- Electromagnetic calorimeter: new trigger optical links
- Hadronic calorimeter: new SiPMS (HO), new PMTs (HF), HF backend (uTCA)
- Drift tube chambers: new trigger electronics
- Resistive plate chambers: new chambers
- Cathode Strip Chamber: bew chambers and electronics
- Silicon pixel: lower temperature (-10 degrees) and recovered channels
- Silicon tracker: lower temperature (-15 degrees)
- Luminosity and beam monitoring: new pixel luminosity telescope, fact beams conditions monitor and beam halo monitor, bril-daq software

2.2.1 CMS coordinate system

The coordinate system used by CMS can be found in Figure 2.5. The origin of the right handed orthogonal coordinate system is chosen to be the point of collisions. The x-axis points towards the centre of the LHC ring such that the y-axis points towards the sky, and the z-axis lies tangent to the beam axis. Since the experiment has a cylindrical shape, customary coordinates are used to describe the momentum $\vec{p}$: the distance ρ, the azimuthal angle $\phi \in [-\pi, \pi]$ - the angle between the x-axis and the projection in the transverse plane of $\vec{p}$ ($\vec{p_T}$) - , the pseudo-rapidity η - expressed by the polar angle θ between the direction of $\vec{p}$ and the beam - :

$$\eta = -\ln\left(\tan\left(\frac{\theta}{2}\right)\right). \tag{2.3}$$

For the energies considered at the LHC, where $E >> m$, the pseudo-rapidity is a good approximation of the rapidity y

$$y = \frac{1}{2}\ln\left(\frac{E + p_z}{E - p_z}\right), \tag{2.4}$$

where the difference of rapidities of two particles is invariant under a Lorentz boost in the z-direction.

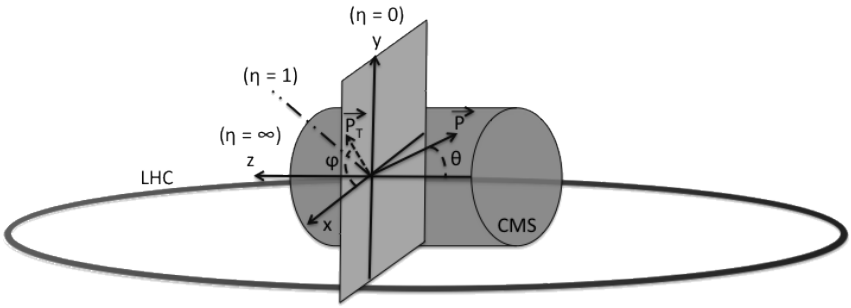

Figure 2.5: Representation of the coordinate system used by CMS. The point of origin is put at the collision point. The x-axis points towards the centre of the LHC ring such that the z-axis lies tangent to the beam axis.

2.2.2 Towards the heart of CMS

The CMS detector consists of two parts; a central barrel around the beam pipe ($|\eta| < 1.4$) and two plugs to ensure the hermeticity of the detector. In Figure 2.6 the onion like structure of the CMS detector is visible. The choice of a solenoid of 12.9 m (FIXME) long and 5.9 m diameter gives the advantage of bending the particle trajectories in the transverse plane. The hadronic calorimeter, the electromagnetic calorimeter and the tracker are within the solenoid, while the muon chambers are placed outside the solenoid.

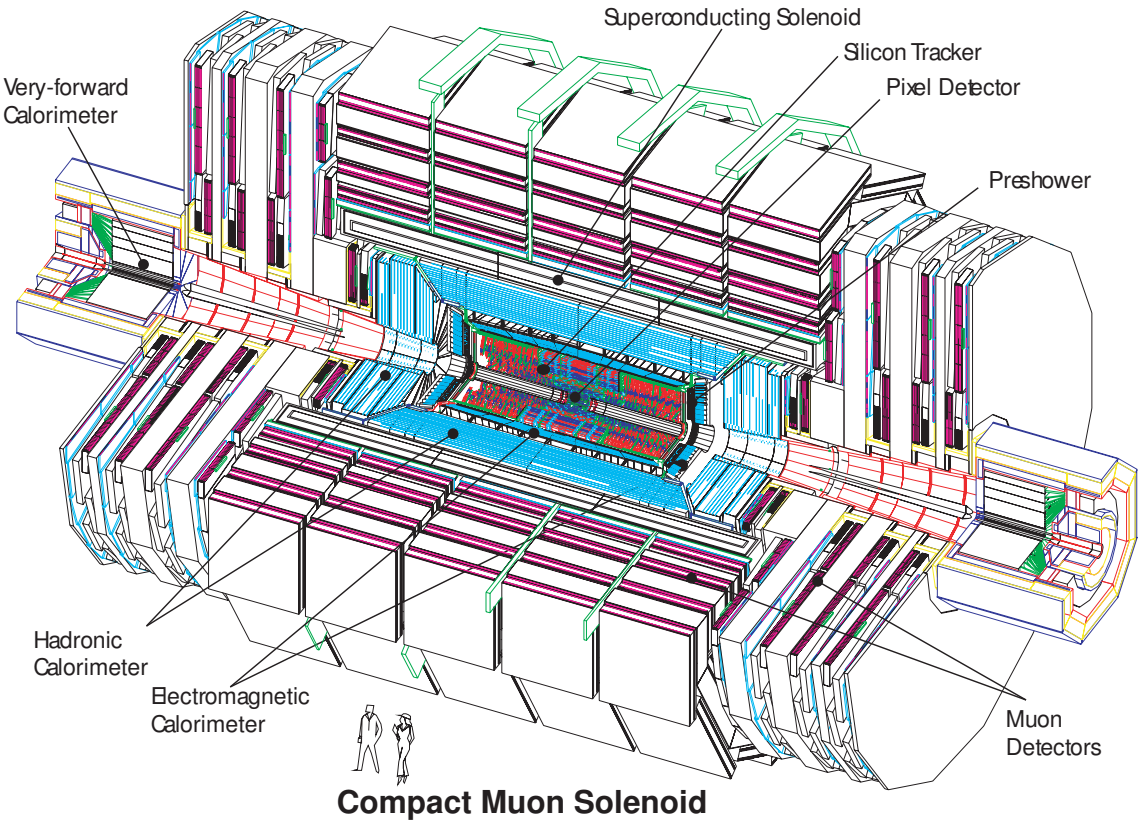

Figure 2.6: Mechanical layout of the CMS detector[22].

2.2.2.1 Muon system

2.2.2.2 Hadronic calorimeter

2.2.2.3 Electromagnetic calorimeter

The electromagnetic calorimeter (ECAL) is designed to measure the energy of photons and electrons and covers $|\eta| < 3$. It consists of 75 848 lead tungstae ($PbWO_4$) crystals. Electromagnetic showers produced by passing electrons or photons ionize the crystal atoms which emit a blue-green scintillation light, that is collected by silicon avalanche photodiodes (APDs) and vacuum phototriodes (VPTs). There are three regions: a central barrel (EB), a endcap region (EE) and a preshower (ES) (Figure 2.7). The relative energy resolution of the ECAL for electrons is between 1.4-3% in EB and 3-4% for EE. In Figure 2.8, the resolutions for low and high bremsstrahlung electrons are shown.

2.2.2.4 Inner tracking system and operations

The tracking system (tracker) [23] is the detecting unit closest to the point of interaction. Responsible for the reconstruction of trajectories from charged particles with $|\eta| < 2.5$, being bend by the magnetic field, it provides a measurement of the momentum. The tracker is also responsible for the determination of the interaction point or vertex. It should be able to provide

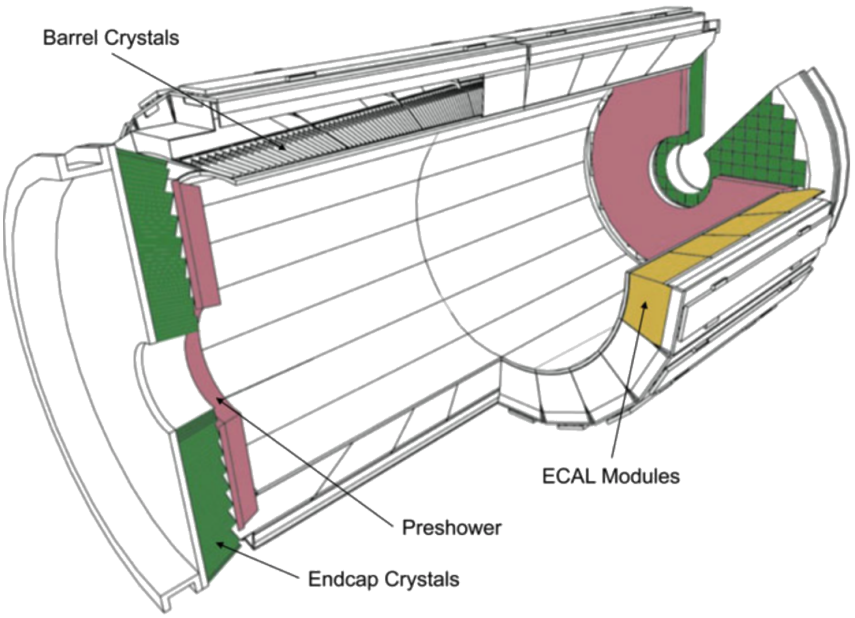

Figure 2.7: Schematic cross section of the electromagnetic calorimeter[11].

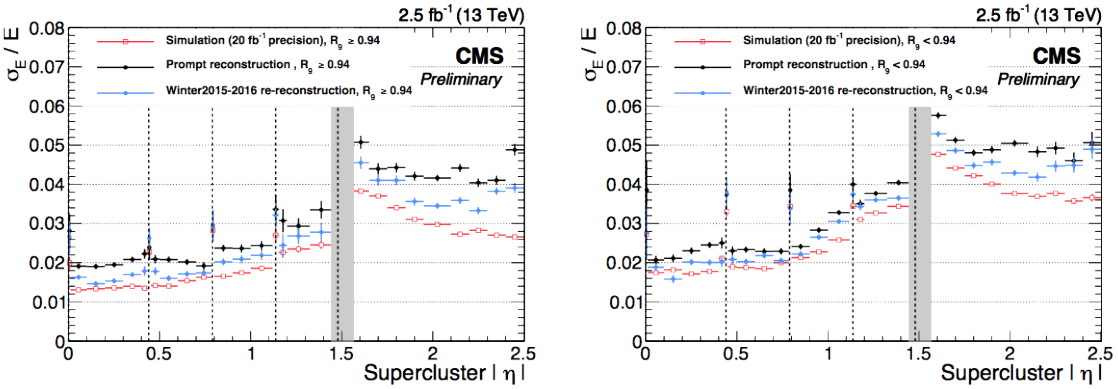

Figure 2.8: Relative energy resolution in bins of pseudo rapidity for the barrel and end caps using electrons from $Z \rightarrow ee$. Left: low bremsstrahlung electrons, Right: high brehmstrahlung electrons[25].

high granularity as well as speed, and be able to endure high radiation. For this reason, the CMS collaboration choose silicon detector technology.

The tracking system consists of a cylinder of 5.8 m long and 2.5 m in diameter. It is immersed in a co-axial magnetic field of 3.8 T due to the solenoid. As shown Figure 2.9, the tracker is built up from a large silicon strip tracker with a small silicon pixel inside. The inner region, pixel ($4.4 < r < 10.2$ cm), gets the highest flux of particles. Therefore, pixel silicon sensors of 100×150 µm is used. It consists of three cylindrical barrels that are complemented by two discs of pixel modules at each side. The silicon strip tracker ($20 < r < 116$ cm) has three subdivisions. The Tracker Inner Barrel and Discs (TIB, TID) are composed of four barrel layers accompanied by three discs at each end. The outer part of the tracker - Tracker Outer Barrel

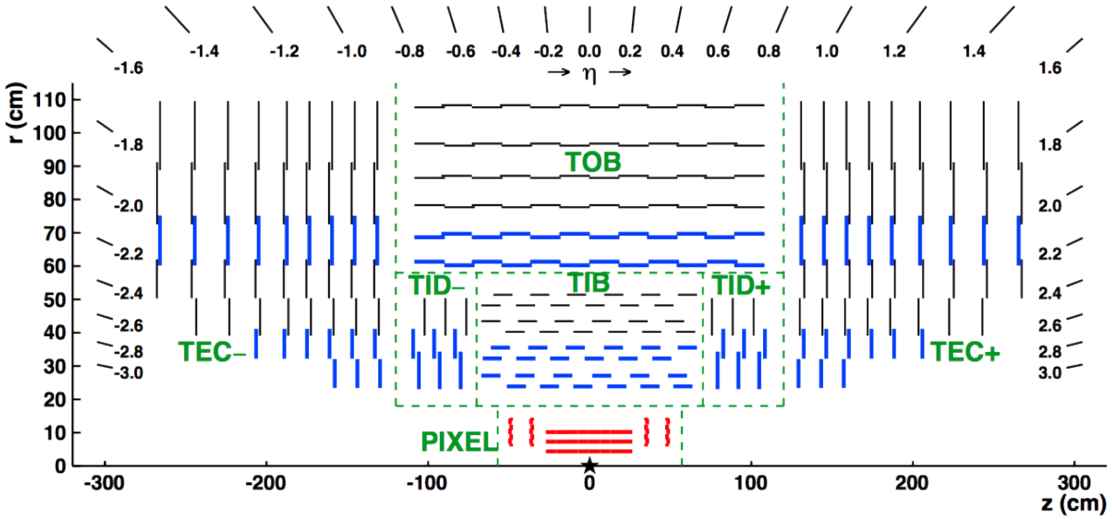

Figure 2.9: Schematic cross section of the top galf of the CMS tracking system in the rz plane. The centre of tracker is shown with a star and corresponds to the approximate position of the proton collision point. The green dashed lines are an indication for each named tracker subsystem. The strip tracker modules that provide two-dimensional hits are shown by thin, black lines, while those able to reconstruct three-dimensional hit positions are shown by thick, blue lines. The pixel modules, shown in red, also provide three-dimensional hits.

(TOB) - consists of 6 barrel layers. In the outer discs, there are nine discs of silicon sensors, referred to as Tracker End Caps (TEC).

The pixel has 1440 modules that cover an area of about 1 m and have 66 million pixels. It provides a three-dimensional position measurement of the hits arising from the interaction from charged particles with the sensors. In transverse coordinate ($r\phi$), the hit position resolution is about 10 µm, while 20-40 µm is obtained in the longitudinal coordinate (z). The sensor plane position provides the third coordinate. The silicon strip trackers consists of 15 148 single sided modules placed in the TIB, TID and the first four rings of the TEC. They provide 9.3 million readout channels. In the TOB and the outer three rings of the TEC, double sided modules are used. These modules are constructed from two back-to-back single sided modules, where one module is rotated through a stereo angle. This covers an active area of about 198 m. The TIB and TID provide position measurements in $r\phi$ with a resolution of approximately 13-38 µm, while the TOB provides a resolution of about 18-47 µm. The resolution in the z direction is approximately 230 µm in the TIB/TID and 530 µm in the TOB. To allow overlay and avoid gaps in acceptance, each module is shifted slightly in r or z with respect to its neighbouring modules within a layer. The resolution on the transverse momentum for a 100 GeV charged particle is abou 2.0% (FIXME), while the impact parameter resolution is about 15 µm. With this detector lay out, at least nine points per charged particle trajectory can be measured in an $|\eta|$ range up to 2.4.

During the first data taking period of the LHC (2010 to 2013), the tracker operated at +4°C. With the higher LHC beam intensities from 2015 onwards, the tracker needs to be operated at much lower temperatures. This is due to the fact with intense irradiation, the

doping concentration changes, the leakage current increases proportional to the fluence and the charge collection efficiency decreases due to charge trapping. Mostly the leakage current (I) is affected by the temperature change:

$$I \propto T^2 e^{-\frac{E_g}{2kT}}, \tag{2.5}$$

where T is the operating temperature, E_g the band gap and k the Boltzmann constant. There is approximatly a factor 15 between the leakage currents at room temperatures and at −10 °C.

During the first long shutdown (LS1), the CMS cooling plant was refurbished[24] and the fluorocarbon cooling system overhauled. To help to suppress the humidity inside the tracker, new methods for vapour sealing and insulation were applied. Furthermore, several hundred high-precision sensors are used to monitor the humidity and temperature. In order to get as dry air as possible, a new dry-gas plant provides eight times more dry gas (air or nitrogen) than during the first run, and allows regulation if the flow. As final addition, the cooling bundels outside the tracker are equipped with heater wires and temperature sensors in order to maintain safe operations. For the data taking in 2015-2016, the tracker operated at −15°C.

Track reconstruction

Primary vertex reconstruction

2.2.3 Data acquisition

2.2.4 CMS computing model

Event generation, simulation and reconstruction

3

3.1 Collision event generation

3.1.1 Parton distribution functions and the hard interaction

3.1.2 Parton showering

3.1.3 Hadronization and decay

3.1.4 Underlying event

3.1.5 Event reconstruction and identification

3.2 Detector simulation

3.3 Physics object reconstruction and identification

3.3.1 The particle flow event reconstruction method

3.3.2 Identification of particles

3.3.2.1 Muon reco and ID

3.3.2.2 Electron reco and ID

3.3.2.3 Jet reco and ID of b quarks

3.3.2.4 Missing transverse energy reconstruction

3.3.3 Calibrations and corrections

The search for FCNC involving a top quark and a Z boson

4

5 Conclusion and outlook

Bibliography

[1] R. Barate et al.: **Search for the standard model Higgs boson at LEP**. In: *Phys. Lett.*, **B565**: (2003), pp. 61–75. doi: 10.1016/S0370-2693(03)00614-2. arXiv: hep-ex/0306033 [hep-ex] (see p. 3).

[2] Kenneth Herner: **Higgs Boson Studies at the Tevatron**. In: *Nucl. Part. Phys. Proc.*, **273-275**: (2016), pp. 852–856. doi: 10.1016/j.nuclphysbps.2015.09.131 (see p. 3).

[3] Abdelhak Djouadi: **The Anatomy of electro-weak symmetry breaking. I: The Higgs boson in the standard model**. In: *Phys. Rept.*, **457**: (2008), pp. 1–216. doi: 10.1016/j.physrep.2007.10.004. arXiv: hep-ph/0503172 [hep-ph] (see p. 3).

[4] Serguei Chatrchyan et al.: **Observation of a new boson at a mass of 125 GeV with the CMS experiment at the LHC**. In: *Phys. Lett.*, **B716**: (2012), pp. 30–61. doi: 10.1016/j.physletb.2012.08.021. arXiv: 1207.7235 [hep-ex] (see p. 3).

[5] Georges Aad et al.: **Observation of a new particle in the search for the Standard Model Higgs boson with the ATLAS detector at the LHC**. In: *Phys. Lett.*, **B716**: (2012), pp. 1–29. doi: 10.1016/j.physletb.2012.08.020. arXiv: 1207.7214 [hep-ex] (see p. 3).

[6] Lyndon Evans and Philip Bryant: **LHC Machine**. In: *Journal of Instrumentation*, **3**:08 (2008), S08001. url: http://stacks.iop.org/1748-0221/3/i=08/a=S08001 (see p. 3).

[7] Thomas Sven Pettersson and P Lefèvre: **The Large Hadron Collider: conceptual design**. Tech. rep. CERN-AC-95-05-LHC. Oct. 1995, p. 20 and 22. url: https://cds.cern.ch/record/291782 (see p. 3).

[8] Jorg Wenninger and Ezio Todesco: **Large Hadron Collider momentum calibration and accuracy**. Tech. rep. CERN-ACC-2017-0007. Geneva: *CERN*, Feb. 2017. url: https://cds.cern.ch/record/2254678 (see p. 4).

[9] Cinzia De Melis: **The CERN accelerator complex. Complexe des accélérateurs du CERN**. In: (July 2016). General Photo. url: https://cds.cern.ch/record/2197559 (see p. 4).

[10] G. Aad et al.: **The ATLAS Experiment at the CERN Large Hadron Collider**. In: *JINST*, **3**: (2008), S08003. doi: 10.1088/1748-0221/3/08/S08003 (see p. 4).

[11] S. Chatrchyan et al.: **The CMS Experiment at the CERN LHC**. In: *JINST*, **3**: (2008), S08004. doi: 10.1088/1748-0221/3/08/S08004 (see pp. 4, 10).

[12] K. Aamodt et al.: **The ALICE experiment at the CERN LHC**. In: *JINST*, **3**: (2008), S08002. DOI: 10.1088/1748-0221/3/08/S08002 (see p. 4).

[13] A. Augusto Alves Jr. et al.: **The LHCb Detector at the LHC**. In: *JINST*, **3**: (2008), S08005. DOI: 10.1088/1748-0221/3/08/S08005 (see p. 4).

[14] M. Bongi et al.: **Astroparticle physics at LHC: The LHCf experiment ready for data taking**. In: *Nucl. Instrum. Meth.*, **A612**: (2010), pp. 451–454. DOI: 10.1016/j.nima.2009.08.039 (see p. 4).

[15] G. Anelli et al.: **The TOTEM experiment at the CERN Large Hadron Collider**. In: *JINST*, **3**: (2008), S08007. DOI: 10.1088/1748-0221/3/08/S08007 (see p. 4).

[16] B. Acharya et al.: **The Physics Programme Of The MoEDAL Experiment At The LHC**. In: *Int. J. Mod. Phys.*, **A29**: (2014), p. 1430050. DOI: 10.1142/S0217751X14300506. arXiv: 1405.7662 [hep-ph] (see p. 5).

[17] Oliver Sim Brüning, Paul Collier, P Lebrun, et al.: **LHC Design Report**. CERN Yellow Reports: Monographs. Geneva: CERN, 2004. URL: https://cds.cern.ch/record/782076 (see p. 5).

[18] Jean-Luc Caron: **Cross section of LHC dipole.. Dipole LHC: coupe transversale.** AC Collection. Legacy of AC. Pictures from 1992 to 2002. May 1998. URL: https://cds.cern.ch/record/841539 (see p. 6).

[19] **Technical proposal**. LHC Tech. Proposal. Cover title : CMS, the Compact Muon Solenoid : technical proposal. Geneva: CERN, 1994. URL: https://cds.cern.ch/record/290969 (see p. 7).

[20] G. L. Bayatian et al.: **CMS physics: Technical design report**. In: (2006) (see p. 7).

[21] G L Bayatian, S Chatrchyan, G Hmayakyan, et al.: **CMS Physics: Technical Design Report Volume 1: Detector Performance and Software**. Technical Design Report CMS. There is an error on cover due to a technical problem for some items. Geneva: CERN, 2006. URL: https://cds.cern.ch/record/922757 (see p. 7).

[22] CMS Collaboration: **Detector Drawings**. CMS Collection. Mar. 2012. URL: https://cds.cern.ch/record/1433717 (see p. 9).

[23] Serguei Chatrchyan, Vardan Khachatryan, Albert M Sirunyan, et al.: **Description and performance of track and primary-vertex reconstruction with the CMS tracker**. In: *J. Instrum.*, **9**:arXiv:1405.6569. CERN-PH-EP-2014-070. CMS-TRK-11-001 (May 2014). Comments: Replaced with published version. Added journal reference and DOI, P10009. 80 p. URL: http://cds.cern.ch/record/1704291 (see p. 9).

[24] **Cool running for CMS tracker**. In: (Mar. 2014). URL: http://cds.cern.ch/record/1998606 (see p. 12).

[25] Menglei Sun: **Achieving the optimal performance of the CMS ECAL in Run II**. Tech. rep. CMS-CR-2016-325. Geneva: *CERN*, Nov. 2016. URL: https://cds.cern.ch/record/2233637 (see p. 10).